Supporting Online Material for

Rise of the Andes

Carmala N. Garzione,* Gregory D. Hoke, Julie C. Libarkin, Saunia Withers, Bruce MacFadden, John Eiler, Prosenjit Ghosh, Andreas Mulch

*To whom correspondence should be addressed. E-mail: garzione@earth.rochester.edu

Published 6 June 2008, *Science* **320**, 1304 (2008)
DOI: 10.1126/science.1148615

This PDF file includes:

Supporting Online Material

Sedimentology and age constraints

The late Oligocene Salla Formation (~29.4 to 24 Ma) (*S1*) was deposited on the west-vergent wedgetop of waning deformation in the western portion of the Eastern Cordillera fold-trust belt (*S2*). These fluvial sandstone and floodplain mudstone units lack contractional deformation features and bracket the age of most shortening in the western portion of Eastern Cordillera to older than ~25 Ma. Well-developed paleosols within floodplain deposits include nodular and bedded pedogenic carbonates and show extensive evidence for root activity, with depths of carbonate formed below 30 to 50 cm. Early Miocene rocks of the Potoco Formation (locally called the Huayllapucara or Totora formations) (*S3, S4*) were sampled within the eastern limb of the Corque syncline near Corque village. Age estimates for these rocks come from biotite K-Ar dates of 23.9 ±1.3 Ma from a tuff within the lower Totora Formation (*S3*). These deposits consist of fluvial sandstones and poorly developed floodplain deposits. Rare paleosols contain small nodules of <0.5 cm diameter formed at depths of 17 to 40 cm.

Middle to late Miocene deposits of the upper Totora through Pomata and lower Umala formations were sampled in 3 sections near Callapa village (Fig. 1) (*S5*). Sanidine $^{40}Ar/^{39}Ar$ from tuffs within the section (*S6*) and magnetostratigraphy (*S5, S7*) provide age constraints for these units. Here, we revise the ages for deposits above the Callapa tuff reported in Garzione et al. (*S5*) based upon a) new $^{40}Ar/^{39}Ar$ plateau ages of 8.60 ± 0.24 Ma and 8.66 ± 0.25 Ma on potassium feldspar and biotite, respectively, from a tuff within our measured section; and b) a more densely sampled magnetic polarity stratigraphy.

Magnetostratigraphy methods

Revision to the magnetostratigraphic section for the 5 to 9 Ma Callapa section published in Garzione et al. (*S5*) is based upon a newly dated tuff and sampling of additional paleomagnetic sites. Today this section sits at elevations between ~3800 and 3900 m, and is bounded by the Callapa tuff and the Toba 76 tuff, radiometrically dated at 9.03 +/- 0.07 Ma and 5.35 +/- 0.003 Ma, respectively (*S6*). A third tuff sampled at a stratigraphic height of 407 m is radiometrically dated in this study at 8.6 ± 0.24 (Table S1) and provides further age constraint on the section. We collected an additional three to four paleomagnetic samples from 21 sites to augment and clarify the magnetostratigraphic correlation reported in Garzione et al. (*S5*) (Table S2). As in that study, samples were demagnetized via thermal demagnetization and had typical unblocking temperatures for characteristic remanent magnetization between 600 and 660ºC. Twenty-one additional samples from 14 sites yielded line-fits with mean angular deviation less than 15º (*S8*). Combining these data with that of Garzione et al. (*S5*), 129 samples from 70 sites provided better constrains on the magnetic reversal stratigraphy. Ambiguity in polarity direction from multiple samples from five sites left 65 sites that were used in correlation with the Geomagnetic Polarity Time Scale (GPTS) (*S9*).

These remaining sites (n=65) were ranked into classes based on data quality (e.g., *S10*) (Table S3). Class A sites contain two or more samples per site with a single polarity within the site and site-mean 95% confidence limit (α_{95}) < 20° (Fig. S1). Class B sites contain two or more samples per site and single polarity within the site, but moderately dispersed ChRM directions (α_{95}> Class A sites, but less than 30º) (Fig. S2). Class C sites contain three samples per site exhibiting multiple polarities. Class D sites have either only one sample per site or two or more with ChRM dispersion far above class B sites (Fig. S3). VGP latitudes were calculated for each of the 65 classified sites using PMag Tools Version 3.2 (*S11*). Class A, B, and C sites are

considered the most reliable data as they had more than one sample representing the site and lower α_{95}. All class A sites were used in the correlation to the GPTS; class B and C sites were used in all cases, except where they disagreed with a higher ranking site. The class D sites occasionally showed disagreement with higher ranked sites and were not directly used in the correlation.

Reversals Test. Site mean directions passed a reversals test (*S12*), performed with the software program PMag Tools, suggesting that the ChRM is primary. Site mean data for class A, B and C sites and the sample data for class D sites passed the Common k Reversal Test (*S13*) with intermediate results. The intermediate classification indicates that the test passed with a high gamma critical (>20), signifying moderate dispersion.

Magnetic Mineralogy. Bulk sample IRM results from ten samples distributed across the section indicate a mixture of magnetite and hematite in the samples (*S14*). The majority of the ChRMs within these samples were stable to temperatures above 600°C, suggesting that the ChRM was carried primarily by hematite (*S15*). Most sample demagnetizations showed a drastic drop in intensity in the earliest temperature steps, which indicates that the dominant mineralogy is less stable. Together, demagnetization and IRM results suggest that the ChRM was carried primarily by hematite. The revised magnetostratigraphic correlation (Fig. S4) results in ages that are slightly younger than ages reported in Garzione et al. (S5) and indicates that the oxygen isotopic shift, inferred to reflect surface uplift, was completed by ~6.3 Ma, instead of 6.8 Ma. This new correlation also requires that a tuff exposed within the Toba 76 section at 223 m is the Callapa tuff (Fig. S4). Although this unit yielded no datable material within the Toba 76 section, the tuff approximately corresponds with the appropriate stratigraphic level and is ~1 m thick, as in the type locality for the Callapa tuff near Callapa village.

Stable isotope methods

Paleosol carbonates were analyzed for their O and C isotopic compositions (Fig. 2, Table S4). Carbonate nodules were examined in thin section and under a binocular microscope. Both Salla samples and Corque samples showed from 10% to 40% sparry recrystallization or sparite infilling of root tubules. Samples were micromilled using a 20 Am drill bit to avoid secondary calcite. Salla samples were analyzed at the University of Arizona using an automated carbonate preparation device (Kiel-III) coupled to a Finnigan MAT 252. Corque samples were analyzed at the University of Rochester using an automated carbonate preparation device (Gasbench II) coupled to a Thermo Electron Delta Plus XL continuous flow instrument. The reported data (Table S4) were obtained by normalizing to the PDB scale by fitting the sample data to a linear correction curve based on three independently determined internal standards and reference materials.

New carbonate 'clumped isotope' analyses made for this study (Table S5) were performed in the Caltech laboratories for stable isotope geochemistry following techniques presented in (*S17*). Samples were prepared by micro-drilling ~10 mg of powder from soil nodules, avoiding secondary sparry calcite where it could be visually identified. Recovered carbonate was reacted with anhydrous phosphoric acid at 25 ˚C overnight, and product CO_2 was purified cryogenically and by passage through a poraplot-Q gas chromatography column held at -10˚C. Purified CO_2 was analyzed on a Thermo Finnegan 253 gas source isotope ratio mass spectrometer that is configured to collect ion beams corresponding to M/Z of 44, 45, 46, 47, 48 and 49. All analyses were standardized for bulk isotopic composition (i.e., $\delta^{13}C$ and $\delta^{18}O$) by comparison with CO_2 prepared from NBS-19 standard using the same techniques and apparatus. Values of Δ_{47} were standardized by comparison with heated gases that are presumed to have

achieved a stochastic distribution of isotopes among all possible isotopologues. All data were corrected for instrument non-linearity in measured 47/44 ratios, as determined by analysis of heated gases that varied dramatically in bulk isotopic composition (i.e., such that known Δ_{47} values of 0 ‰ could be observed over a range of 47/44 ratios). Analyses containing evidence of clear contamination on masses 48 and/or 49 were rejected.

These data were generated with the purpose of surveying Oligocene to early Miocene Altiplano soil carbonates to determine whether they preserve temperatures within error of earth surface conditions, or were reset to higher burial metamorphic temperatures (*S18*). This purpose could be fulfilled with relatively poor precision, and so analytical durations for these measurements were substantially less than in previous clumped isotope work aimed at altimetry or climate reconstructions. Each analysis represents the average of 3-5 acquisitions (average 4), for a total sample collection time of 240-400 s (average 320 s), and only one sample was externally replicated through separate gas extractions. A similar level of replication was made for accompanying analyses of heated gas standards. Counting-statistics errors (i.e., shot noise) for this level of replication are ±0.021 ‰, 1s — four times higher than typical of this technique (e.g., *S19, S20*). Furthermore, the heated gases analyzed over the course of generating this data set varied by about twice than expected from counting statistics alone, suggesting unresolved fluctuations in the heated reference gases over this period. We have included this variability in the heated gas reference materials to our total error estimate. Therefore, our external error estimate for sample Δ_{47} values averages 0.043 per mil — 8 times the average value from recent studies focused on paleoclimate and paleoaltimetry (e.g., *S19, S21*). The one sample analyzed in triplicate (02BSC5) yielded an external error of ± 0.040 ‰, suggesting our error estimate for each measurement is appropriate.

Bulk clay minerals (smectite) from weathered silicic ashes were separated from individual waterlain tuffs within the section sampled for oxygen isotope stratigraphy of pedogenic carbonates. Individual tuffs were ground by mortar and pestle. About 60-100g of sample were stirred for 1 hour in a solution of Na-pyrophosphate and deionized water. Clay mineral concentrates were obtained by standard settling and centrifuge techniques. The <1.0 μm grain size fraction was purified and dried at 70°C for 20 days under vacuum prior to isotopic analysis. Hydrogen isotopic compositions were measured by continuous flow GC-IRMS using a thermal combustion elemental analyzer attached to a ThermoFinnigan delta+XL mass spectrometer. About 0.8 to 1.0 mg of clay separates were wrapped into Ag-foil and heated to 1450°C in a glassy carbon reduction furnace thereby liberating hydrogen. Measurements were duplicated for each sample. Results were highly reproducible and precision of δD_{clay} was ±2‰. The final data (Fig.2, Table S6) were obtained by first normalizing raw data to a common signal size, and then normalized to the SMOW scale by fitting the sample data to a linear correction curve based on four or five independently determined standards and reference materials. This correction curve is generated daily by plotting the measured δD value of these reference materials against their certified δD value. Following that procedure NBS-30 and NBS 22 yielded δD values within uncertainty of the referenced values.

References

S1. R. F. Kay, B. J. MacFadden, R. H. Madden, H. Sandeman, F. Anaya, *J. Vertebrate Paleont.***18**, 189 (1998).
S2. N. McQuarrie, P. DeCelles, *Tectonics* **20**, 669 (2001).
S3. L. Kennan, S. Lamb, C. Rundle, *J. South Am. Earth Sci.* **8**, 163 (1995).
S4. B. K. Horton, P. G. DeCelles, *Basin Research* **13**, 43 (2001).
S5. C. N. Garzione, P. Molnar, J. C. Libarkin, B. J. MacFadden, *Earth Planet. Sci. Lett.* **241**, 543 (2006).
S6. L. G. Marshall, C. C. Swisher, III, A. Lavenu, R. Hoffstetter, G. H. Curtis, *J. South Am. Earth Sci.* **5**, 1 (1992).

S7. P. Roperch, G. Herail, M. Forani, *J. Geophys. Res.* **104**, 20415 (1999).
S8. J. L. Kirschvink, *Geophys. J. Royal Astronom. Soc.* **62**, 699 (1980).
S9. S. C. Cande, D. V. Kent, *J. Geophys. Res.* **100**, 6093 (1995).
S10. T. P. Ojha *et al.*, *Geol. Soc. Am. Bull.* **112**, 424 (2000).
S11. M. W. Hounslow. (Lancaster, United Kindom, 2003).
S12. P. L. McFadden, M. W. McElhinney, *International J. Geophys.* **103** (1990).
S13. P. L. McFadden, F. J. Lowes, *Geophys. J. Royal Astronom. Soc.* **67**, 19 (1981).
S14. D. H. Tarling, *Palaeomagnetism: Principles and Applications in Geol., Geophys. and Archaeol.* (Chapman and Hall Ltd., New York, New York, 1983).
S15. R. F. Butler, *Magnetic Domains to Geologic Terranes* (Blackwell Scientific Publications, Cambridge, MA, 1992), pp.
S16. D. R. Gray, D. A. Foster, B. Goscombe, C. W. Passchier, R. A. J. Trouw, Precambrian Research **150**, 49 (2006).
S17. P. Ghosh, J. Adkins, H. Affek, B. Balta, W.F. Guo, E.A. Schauble, D. Schrag, J.M. Eiler, *Geochim. et Cosmochim. Acta* **70**, 1439 (2006).
S18. J. Eiler, C. Garzione, P. Ghosh, *Science* **314**, 760c (2006).
S19. R.E. Came, J.M. Eiler, J. Veizer, K. Azmy, U. Brand, C.R. Weidman, *Nature* **449**, doi:10.1038/nature06085 (2007).
S20. H. Affek, J.M. Eiler, Geochim. et Cosmochim. Acta **70,** 1 (2006).
S21. P. Ghosh, C. N. Garzione, J. M. Eiler, *Science* **311**, 511 (2006).
S22. S. Withers, Ohio University (2006).

Figures

Figure S1. Sample from Class A site. a) Vector component diagram, tick marks equal 100mA/M, inset tick marks equal 10mA/M. All vector component diagrams were generated using SuperIAPD (*S12*); b) IRM acquisition curve for sample from same site.

Figure S2. Sample from Class B site, tick marks equal 1mA/M; b) IRM acquisition curve for sample from same site.

Figure S3. Sample from class C or D site, tick marks equal 10mA/M; b) IRM acquisition curve for sample from same site.

Figure S4. Revised magnetostratigraphic correlation. Stratigraphic level of dated tuffs (*S6*) and the new tuff age reported here are shown. B. Correlation of magnetic polarity stratigraphy to geomagnetic polarity time scale (*S9*). Site-means of virtual geomagnetic pole (VGP) plotted versus stratigraphic level above the Callapa tuff. Positive VGP latitude indicates normal polarity, shown as black intervals; negative latitude indicates reversed polarity shown as white intervals. The site mean data used in the correlation are connected with the black line, black circles are class A sites, gray circles are class B, open circles are class C, and open triangles are class D (following *S10*).

Table S1. Summary of $^{40}Ar/^{39}Ar$ data from mineral separates.

Sample Name	Sample Type	% gas used to calculate plateau ages	Age (Ma) ± 2 σ
03BL47a	biotite, weighted plateau age	90% of ^{39}Ar released	8.66 ± 0.26
03BL47b	K feldspar, weighted plateau age	60% of ^{39}Ar released	8.60 ± 0.24

Mineral separates are from a tuff at level 407 m in the Toba 76 section (*S5*). Mineral separations were carried out by Apatite to Zircon, Inc. Analyses were done at the University of Florida using methods discussed in (*S16*).

Table S2. Total number of samples collected and sites utilized in study (from *S22*).

sampling trips	samples collected	sampled sites	sites picked	samples discarded (high MAD)	Sites discarded (ambiguity)	total samples	total sites
2004 field season	173	56	46	10	3	89	44
2005 field season	90	30	24	9	2	31	21
total	263	86	70	19	5	120	65

Table S3. Site mean ChRM and VGP data, corrected for strike and dip of bedding at study site locality (S17°37', W68°18') (from *S22*).

site	strat. height	total # samples	sample polarity	site rank	site mean declination	site mean inclination	colatitude	VGP latitude
1	6.6	3	**rrr**	B	297.3	-19.5	-79.96	-28.89
2	23.6	2	**nn**	B	147.8	-18.3	-80.61	48.28
3	56.7	2	**rr**	B	166.5	4.3	87.85	-69.65
4	92.8	0	--	--				
5	110	3	**nn**	B	154.3	-23.1	-77.96	50.98
6	129.5	2	**nr**	--	161.6	-4.2	-87.90	63.22
7	147.8	3	**rrn**	C	160.4	6.4	86.79	-65.99
8	166.2	2	**nn**	A	328.3	32.2	72.52	43.06
9	187.4	2	**rr**	B	161.3	5.3	87.34	-66.34
10	206.3	1	**r**	D	290.01	-59.52	-49.65	-26.38
11	219.7	1	**r**	D	312.53	-0.54	-89.73	-40.22
12	250.4	0	--	--				
13	272	0	--	--				
14	288.6	0	--	--				
15	309.3	2	**rr**	B	2	32.1	72.59	54.93
16	321	2	**rn**	D	270.17	45.9	62.71	-7.82
17	370.2	3	**nnn**	A	334.7	19.7	79.85	52.65
18	388.1	2	**nn**	A	345.7	2.8	88.60	66.35
19	406	3	**rrr**	B	349.7	-13.3	-83.26	-75.20
20	416.3	3	**rnn**	C	299.1	51.2	58.12	13.53
21	442.5	2	**nn**	B	325.9	23.9	77.51	44.85
22	463.5	0	--	--				
105	464	2	**rrr**	B	196.1	45.6	62.95	-72.39
104	471	1	**n**	D	351.73	14.02	82.88	63.97
103	479	1	**r**	D	357.37	-0.56	-89.72	-72.49
23	482.8	2	**rr**	B	356.9	-30.1	-73.84	-86.70
102	489	0	--	--				
101	500	2	**nr-**	--	158.7	33.9	71.43	-69.74
24	501.2	1	**r**	D	25.67	-38.39	-68.39	-65.52
100	509	1	**r**	D	348.32	-16.27	-81.70	-75.31
25	524.5	0	--	--				
26	543	2	**nn**	B	140.7	-4.8	-87.60	46.41
27	561.2	1	**n**	D	181.85	-1.79	-89.10	71.42
28	581.3	0	--	--				
29	601.2	3	**rnr**	C	338.8	-16.9	-81.36	-67.52
30	623.5	2	**rr**	A	138.6	5.4	87.29	-46.76
31	642.4	1	**n**	D	179.92	-21.21	-79.02	61.42
127	654	0	--	--				
32	662.1	3	**nnn**	A	146.6	-13.6	-83.10	48.91
126	662	0	--	--				
125	665	1	**n**	D	175.7	-10.63	-84.64	66.65
33	684.3	1	**n**	D	170.55	-33.51	-71.68	52.90
124	689	1	**n**	D	34.66	33.25	71.85	40.60
123	702	0	--	--				

34	704.9	1	**n**	D	10	10.88	84.51	64.89
122	712	2	**nn**	B	334.1	42	65.76	41.13
35	719	1	**r***	D	274.76	42.04	65.73	-2.99
121	725	0	--	--				
120	732	0	--	--				
36	734	3	**nnn**	B	353.9	10.3	84.81	66.43
119	750	3	**nnn**	B	334	21.9	78.64	51.29
37	758.9	2	**n-n-**	A	326.4	2.6	88.70	51.89
118	761	1	**r-**	D	316.59	-12.24	-83.81	-46.14
117	772	3	**nn-n**	A	1.6	8	85.98	68.32
38	784.6	3	**nnn-**	A	350.8	13.6	83.10	63.87
116	790	1	**r-**	D	192.56	26.47	76.02	-77.39
39	801.3	1	**r**	D	15.11	-4.36	-87.82	-68.60
115	802	1	**r-**	D	133.27	3.27	88.36	-41.43
114	813	3	**rrr**	B	130	8.5	85.73	-39.31
113	820	1	**r**	D	333.75	-18.33	-80.59	-63.23
40	822.9	3	**nnn**	A	341.1	7.9	86.03	61.49
112	837	2	**n**	D	299.36	28.64	74.73	21.79
41	840.7	3	**nnn**	A	329.2	2.5	88.75	54.29
42	864.2	0	--	--				
111	856	1	**r**	D	334.29	-32.33	-72.44	-65.51
110	871	1	**n**	D	334.87	16.54	81.55	54.02
43	884.5	3	**rrr**	A	351.6	-6.5	-86.74	-73.46
109	886	1	**r***	D	105.37	-73.38	-30.84	-7.48
44	901.1	1	**r**	D	136.62	18.81	80.33	-47.20
108	909	1	**r**	D	129.98	18.1	80.72	-40.78
45	924.4	1	**n**	D	156.48	-10.6	-84.65	57.35
107	933	0	--	--				
106	946	0	--	--				
46	948.5	2	**nn**	B	207.4	-32.4	-72.40	45.66
47	967.1	2	**rn**	D	165.33	-14.87	-82.44	60.96
48	987	1	**n**	D	0.28	47.97	60.98	43.38
49	1004.6	1	**n**	D	151.86	-1.39	-89.30	56.80
50	1027.5	1	**r**	D	172.91	9.37	85.28	-75.37
51	1047	3	**nnn**	B	152.3	-6	-86.99	55.78
52	1066.5	3	**nnr**	C	188.8	-10.2	-84.86	65.66
53	1082.5	2	**rr**	A	165.2	6.3	86.84	-69.53
54	1105.3	3	**rrr**	A	172.4	20.4	79.47	-79.79
55	1121.5	3	**rr**	A	11	-16.4	-81.63	-75.87
129	1121.5	1	**r**	D	349.46	-14.55	-82.61	-75.52
128	1160.5	2	**rr**	A	340	-25.6	-76.53	-70.31
56	1162.9	2	**rn**	X	10.6	-5.7	-87.14	-71.96

Sites 1-56 were sampled in 2004; sites 100-129 were sampled in 2005. n is normal, r is reversed. Site rank as described in text.

Table S4. Oxygen and carbon isotope data from late Oligocene to early Miocene pedogenic carbonates samples near Salla and Corque.

Sample name	GPS location, elevation (m)	approximate age	$\delta^{18}O$(VPDB) (‰)	$\delta^{13}C$(VPDB) (‰)
Salla				
02BS2	sampled above 02BS2,	25.5	-7.2	-9.2
02BS3	S17º11.20', W67º36.94', 3834	25.7	-6,2	-8.9
02BS4	sampled between 02BS3	26.0	-8.2	-9.5
02BS5	S17º11.21', W67º36.04', 3821	27.8	-7.4	-8.4
02BS6	S17º11.21', W67º36.04', 3829	28.0	-7.1	-8.3
02BS7	S17º11.21', W67º36.04', 3827	28.2 -	-6.6	-8.1
Corque				
05BL44	S18º20.88', W67º41.58', 3904	23.6	-7.1	-7.5
05BL40	S18º20.94', W67º41.44', 3914	23.7	-9.4	-8.4
05BL39	S18º20.98', W67º41.42', 3910	23.8	-8.8	-8.0
05BL35	S18º20.98', W67º41.39', 3895	24.5	-12.1	-8.7

Analytical uncertainties on $\delta^{18}O$ and $\delta^{13}C$ (not shown) are less than ±0.1 and ±0.06‰, respectively. VPDB – Vienna Peedee belemnite. Ages are approximated based on position in stratigraphic section relative to datums of known age (*S1, S3*). See text for discussion.

Table S5. Δ_{47} data from late Oligocene to early Miocene pedogenic and lacustrine carbonates samples near Salla, Corque, and Tambo Tambillo.

Sample	Age (Ma)	$\delta^{13}C_{PDB}$ of carbonate	$\delta^{18}O_{PDB}$ of carbonate	Δ_{47} of extracted CO_2	Temperature (°C)	Nature of sample
Salla						
02BSC2	25.5	-9.14	-7.15	0.556 (42)	47.7 (10.7)	paleosol
02BSC5	26.5	-8.48	-7.52	0.643 (41)	25.8 (10.5)	paleosol
02BSC5*	26.5	-9.14	-7.15	0.570 (43)	43.8 (10.8)	paleosol
02BSC5*	26.5	-8.31	-7.42	0.577 (42)	41.9 (10.6)	paleosol
05BSC7	28.5	-8.38	-6.87	0.557 (43)	47.4 (10.9)	Paleosol
Corque						
05BL44	23.6	-7.53	-8.34	0.617 (41)	31.9 (10.4)	paleosol
Tambo Tambillo						
05BL49	25	-3.83	-10.04	0.563 (44)	45.9 (11.8)	lacustrine
05BL50	24.5	-2.77	-6.15	0.654 (43)	23.27 (11.0)	lacustrine
05BL53	23.5	-3.00	-11.10	0.539 (45)	52.9 (11.4)	lacustrine
05BL56	23.5	-3.48	-10.00	0.572 (43)	43.31 (11.0)	lacustrine

* repeat analyses. Within run precision on $\delta^{18}O \leq \pm 0.1$ and $\delta^{13}C \leq \pm 0.06$‰. VPDB Vienna Peedee Belemnite. Analytical uncertainties in Δ_{47} (numbers in parentheses) are shown for each measurement as the standard error of the mean of all mass spectrometric analyses for a given sample. These are propagated to estimate uncertainties in temperature (numbers in parentheses). Ages are approximated based on position in the stratigraphic section relative to datums of known age (*S1, S3*). See text for discussion. Locations for Salla and Corque samples are shown in Table S4. Tambo Tambillo samples were collected at S19º28.53', W67º20.30', elev. = 3755 m.

Table S6. H isotope data from authigenic clay in late Miocene volcanic ash deposits.

Sample name	Stratigraphic level (m)	age (Ma)	δD (‰)
05BL2	436	8.32	-119
05BL3	442	8.26	-123
05BL4	449	8.20	-114
05BS5	474	7.96	-118
05BL6	492	7.79	-120
05BS7	493	7.78	-123
05BL8	529	7.43	-117
05BL24	536	7.37	-114
05BL23	583	6.92	-112
05BL21	644	6.57	-109
05BL20	653	6.55	-119
05BL19	654	6.55	-124
05BL18	664	6.54	-126
05BL17	704	6.48	-120
05BL16	712	6.47	-118
05BL15	726	6.45	-119
05BL12	848	6.27	-126
05BL11	852	6.27	-127
05BL10	854	6.27	-124
05BL30	985	6.03	-124
05BL31	987	6.03	-124
05BL25	1160	5.30	-131
05BL27	1220	4.88	-131
05BL28	1220.2	4.88	-121

Volcanic ash samples were collected within the Toba 76 section (*S5*). Ages are derived by linear extrapolation from the magnetic reversal stratigraphy reported here.

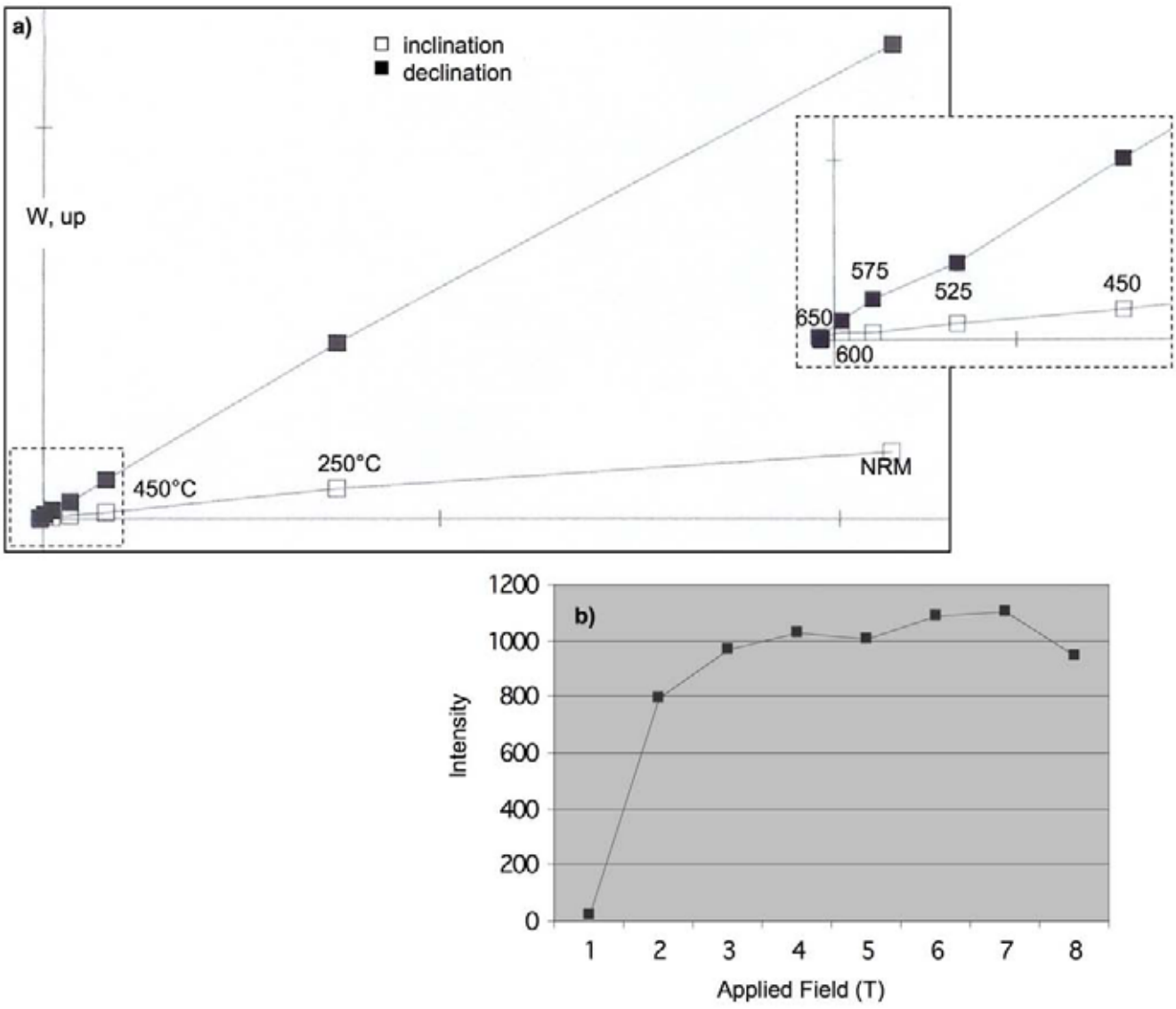

Supplementary Figure 1, Garzione et al.

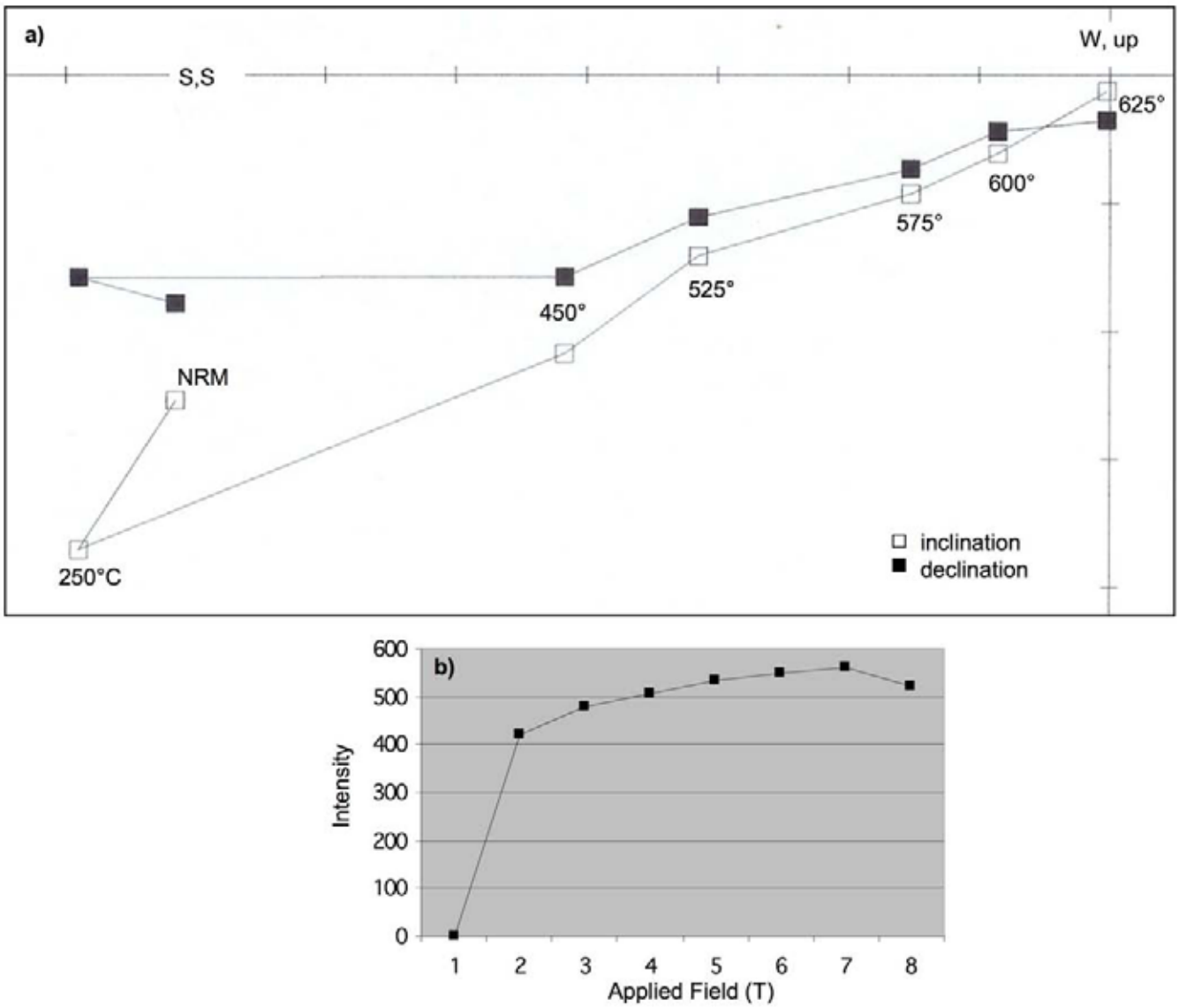

Supplementary Figure 2, Garzione et al.

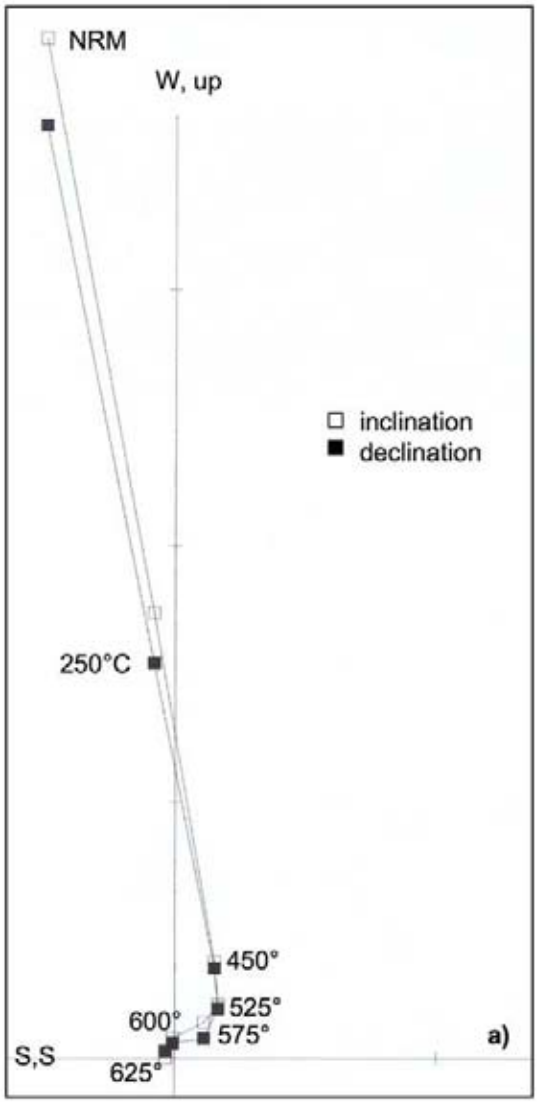

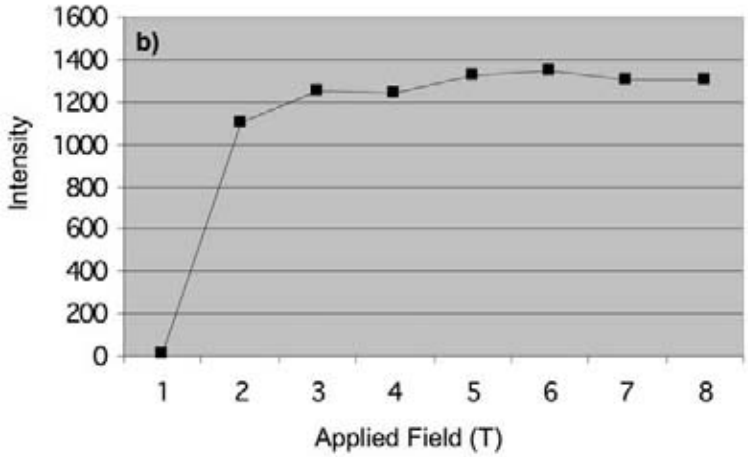

Supplementary Figure 3, Garzione et al.

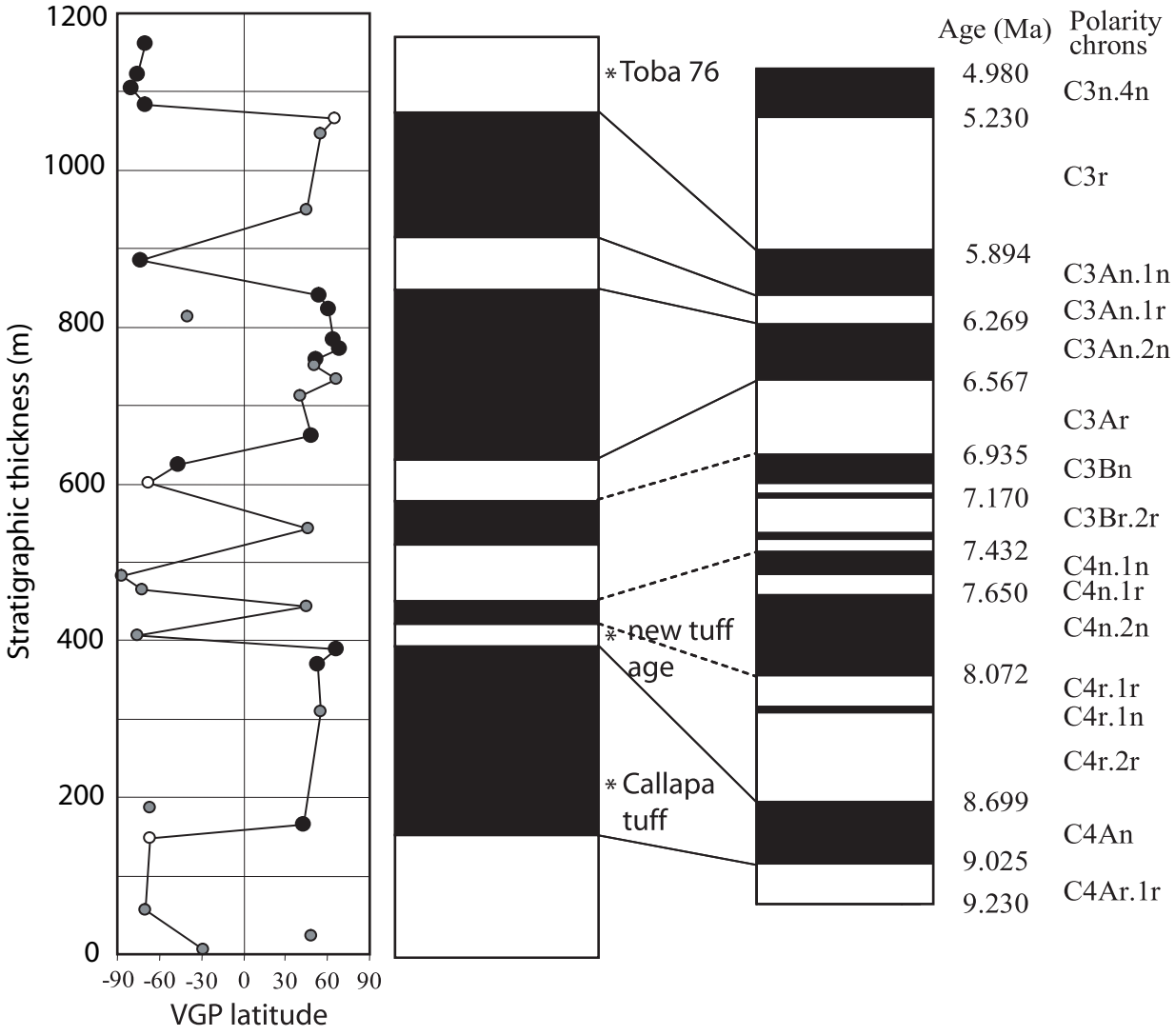

Garzione et al., Supplementary Figure 4